



Corrosion Protection of AISI 304 Stainless Steel using Thin Films of Manganese Nitride

Fatemeh Abdi

Department of Engineering Sciences, Faculty of Advanced Technologies, University of Mohaghegh Ardabili, Namin, Iran

(Received 22 Feb. 2021; Final revised received 18 Jun. 2021)

Abstract

In this work, the thin films of manganese nitride were used to protect AISI 304 stainless steel against corrosion in 3.5% salt solution. These coatings were prepared using the physical vapor deposition of manganese. After deposition, the samples were placed in a furnace under nitrogen flux for nitriding. The crystal structure of the samples was studied using X-ray diffraction (XRD) pattern, and the formation of manganese nitride phase was observed. An atomic force microscope (AFM) was used to investigate the surface morphology of the samples. To evaluate the corrosion resistance of the structures, EIS and polarization tests were performed on the samples. the corrosion resistance of the samples was obtained by simulating the equivalent circuit. Finally, the surface of the corroded samples was observed using scanning electron microscopy (SEM).

Keywords: AISI 304 SS, Corrosion, Manganese Nitride, EIS, Equivalent circuit.

Introduction

Steel has many applications in industry and technology due to its good mechanical properties and good corrosion resistance. However, in the presence of environments containing Cl⁻ and S²⁻ ions, this material does not have good resistance [1-3]. Therefore, improving the corrosion resistance of this widely used material is very necessary. So far, many methods have been used to increase the corrosion resistance of steel. Older methods such as painting have been widely used due to the good adhesion of paint to steel [4]. Today, various methods such as ion implantation [5], arc ion plating [6], sol-gel coating [7,8], chemical coating [9] and physical coating [5,10, 11] are used to reduce the thickness of the coating. The advantage of physical vapor deposition is the controllability of the obtained coating properties as well as its high degree of purity. In recent years, researchers have used different coatings to increase corrosion resistance using the physical vapor deposition method [12-21]. For corrosion protection of metals, it is necessary to investigate the corrosion theory. It is well known that matter is corroded when it loses electrons in a corroding medium. Therefore, for corrosion protection of metals, the tendency and rate of electron loss must be controlled. Since the tendency and speed of electron loss is controlled by electrical impedance, electrical impedance must be increased to increase the corrosion resistance. Electrical impedance is an imaginary quantity that is represented by the following equation:

$$Z = Z' + iZ'' \quad (1)$$

The real and imaginary part of electrical impedance depends on the type and geometry of the material, and is written in one of the following forms:

A: If there is a complete coating on the material surface and this structure is exposed to a corrosive environment, this material is considered as a capacitance (C) parallel to a resistance (R_p). This capacitance is called a double layer capacitance and is displayed with C_d. If we consider the resistance of the solution as R_s, the electrical impedance is written as follows:

$$Z = R_s + \frac{1}{\frac{1}{R_p} - i\omega C} = R_s + \frac{R_p}{1 + \omega^2 R_p^2 C^2} - i \frac{\omega R_p^2 C}{1 + \omega^2 R_p^2 C^2} \quad (2)$$

B: For an incomplete coating, that has porosity and the solution can penetrate into it, another capacitance (C_{cot}) is considered parallel to the resistance in electrical impedance. In this case the electrical impedance is written as follows:

$$Z = R_s + \frac{1}{\frac{1}{R_1} - i\omega C_{cot}} + \frac{1}{\frac{1}{R_2} - i\omega C_d} = R_s + \frac{R_1}{1 + \omega^2 R_1^2 C_{cot}^2} + \frac{R_2}{1 + \omega^2 R_2^2 C_d^2} - i\left(\frac{\omega R_1^2 C_{cot}}{1 + \omega^2 R_1^2 C_{cot}^2} + \frac{\omega R_2^2 C_d}{1 + \omega^2 R_2^2 C_d^2}\right) \quad (3)$$

C: If the invasive ions of the corrosive solution make a hole in the coating, inductance (L) behavior is also seen and the impedance is written as follows:

$$Z = R_s + \frac{1}{\frac{1}{R_p} + \frac{1}{-i} + \frac{1}{i\omega L + R_L}} = R_s + \frac{R_p(R_L^2 + \omega^2 L^2)(R_L^2 + \omega^2 L^2 + R_p R_L)}{(R_L^2 + \omega^2 L^2 + R_p R_L)^2 + (\omega C R_p(R_L^2 + \omega^2 L^2) - \omega L R_p)^2} - i \frac{R_p(R_L^2 + \omega^2 L^2)(\omega C R_p(R_L^2 + \omega^2 L^2) - \omega L R_p)}{(R_L^2 + \omega^2 L^2 + R_p R_L)^2 + (\omega C R_p(R_L^2 + \omega^2 L^2) - \omega L R_p)^2} \quad (4)$$

Due to the fact that the electrical impedance depends on the resistance, capacitance, and inductance, so to increase the electrical impedance, the resistance must increase, the capacitance must decrease, and inductive behavior disappears. Due to the fact that these elements are related to the material type and geometry of the coating, by changing the surface material and surface geometry, the impedance and corrosion resistance can be increased [22-26]. In recent years, using a physical vapor deposition method, and the formation of manganese nitride thin film on AISI 304 stainless steel are reported to greatly increase the corrosion resistance of steel [27-30]. The purpose of this work is to investigate the morphology effect on the corrosion resistance, for which we used two-layer structures. In fact, by converting a single-layer coating to a two-layer coating, by changing the grain size of the coating, the change in electrical impedance is investigated.

Experimental

Sheets of 304 steel in the dimensions of 20mm × 20mm × 1mm with the compounds listed in Table 1 were considered as substrates.

Table 1. Chemical composition of AISI 304 type stainless steel used in this work.

Element (wt%)				
Mn	Ni	Cr	Si	C
1.62	8	18.34	0.34	0.07

To begin with, the sheets were first cleaned in acetone and then in alcohol in the ultrasonic bath and glued to the substrate holder with a special vacuum adhesive. Manganese was considered as the initial material and the deposition was performed, using the Edward coating machine and by the electron beam, at room temperature and base pressure of $\gamma \times 10^{-7}$ Torr in two stages. The first time, a thin layer of manganese with a thickness of 110 nm was formed on the AISI 304 stain less steel, but the second time, the coating layer was done in two steps, so that first a thin layer of manganese with a thickness of 55 nm was deposited on the AISI 304 stain less steel and after a half hour break, another 55 nm was placed on the previous layer. The total thickness of the manganese thin film on stainless steel was 110 nm. The purpose of the half hour interruption was to cool the previous layer and stabilize the grains. After deposition of monolayer and bilayer structures of manganese on AISI 304 stain less steel, nitriding was performed using a furnace (Exciton, 1200-30 / 6, T.H, Iran, equipped with Shinko temperature programmable controller - PCD33A). To do this, the samples were annealed at 623 K with a flow rate of 400 sccm. The annealing process consisted of three steps:

A: It took an hour for the temperature to reach 623 K (at a rate of 6 degrees per minute).

B: The samples were kept at this temperature for 4 hours.

A: The device was turned off to bring the temperature slowly from room temperature 623 K to room temperature.

In all the above steps, the nitrogen flux passed through the samples. To ensure the formation of manganese nitride phase, and to investigate the crystalline degree of the samples, XRD analysis was performed (CuK radiation; 40 kV, 30 mA) with a step size of 0.02° and count time of 1s/step. Cross section of the mono layer and bi layer thin films were observed by means of field emission scanning microscope (FESEM: Hitachi S-4100 SEM, Japan) images and the morphology of the obtained samples was examined using an atomic force microscope (AFM: Auto Probe Pc, Park Scientific Instrument, USA; in non-contact mode, with low stress silicon nitride tip of less than 200\AA radius and tip opening of 18°).

Polarization test was performed to evaluate the corrosion rate and corrosion tendency and corrosion resistance of various structures. This was done using a 3-electrode cell and a company-made model potentiostat device. The 3.5% NaCl solution was considered as a corrosive solution. AgCl solution and platinum electrode were used as reference electrode and auxiliary electrode, respectively. The samples were placed in the fixture as a working electrode in such a way that only a circle with a diameter of 1 cm of the samples was exposed to the corrosive environment. Polarization test was measured with a potential start of -0.5 V to 0.5V, with a rate of 50mV /s . EIS test was performed in the frequency range of 0.01 Hz to 100000 Hz and with a voltage Amplitude of 0.01V. Prior to

measurement, the samples were immersed in solution for 0.5 h to stabilize the potential. After corrosion testing, SEM images were taken from the samples to observe the surface.

Results and discussions

AFM and FESEM analysis

FESEM images were used to observe the cross section of the monolayer and bilayer manganese nitride thin films. Figures (1- a) and (1-b) show the FESEM images of monolayer and bilayer manganese nitride structures, respectively.

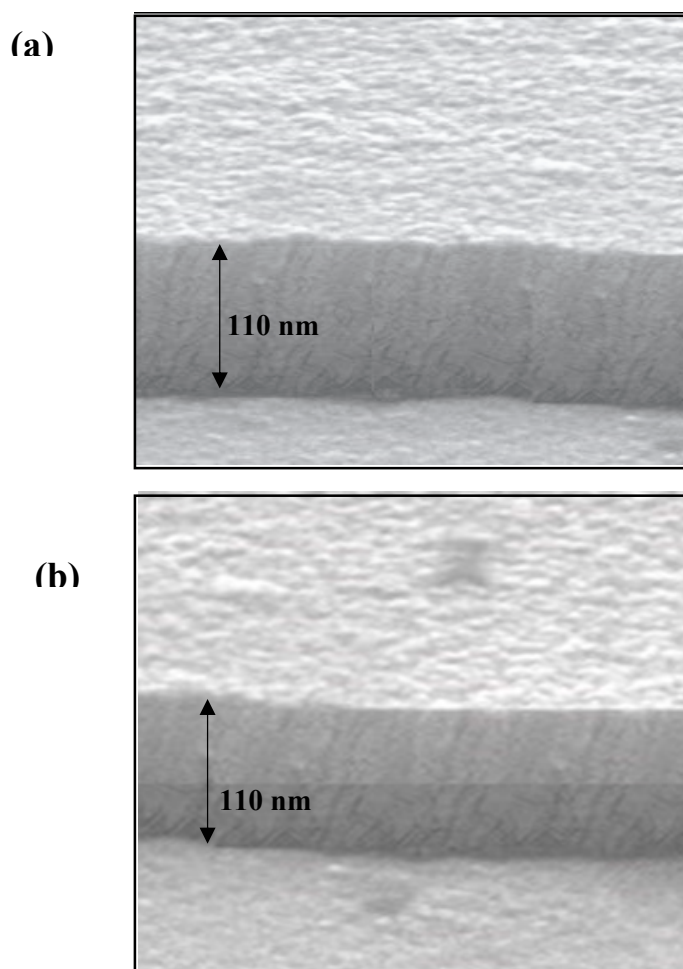


Figure 1. FESEM images of manganese nitride thin films. a) monolayer and b) bilayer.

The surface morphology of these structure after annealing processes, were examined using an atomic force microscope (AFM). Figure 2 shows the two and three-dimensional images of these thin films. It is clear from the figure that the bilayer sample has smaller grain sizes than monolayer structure.

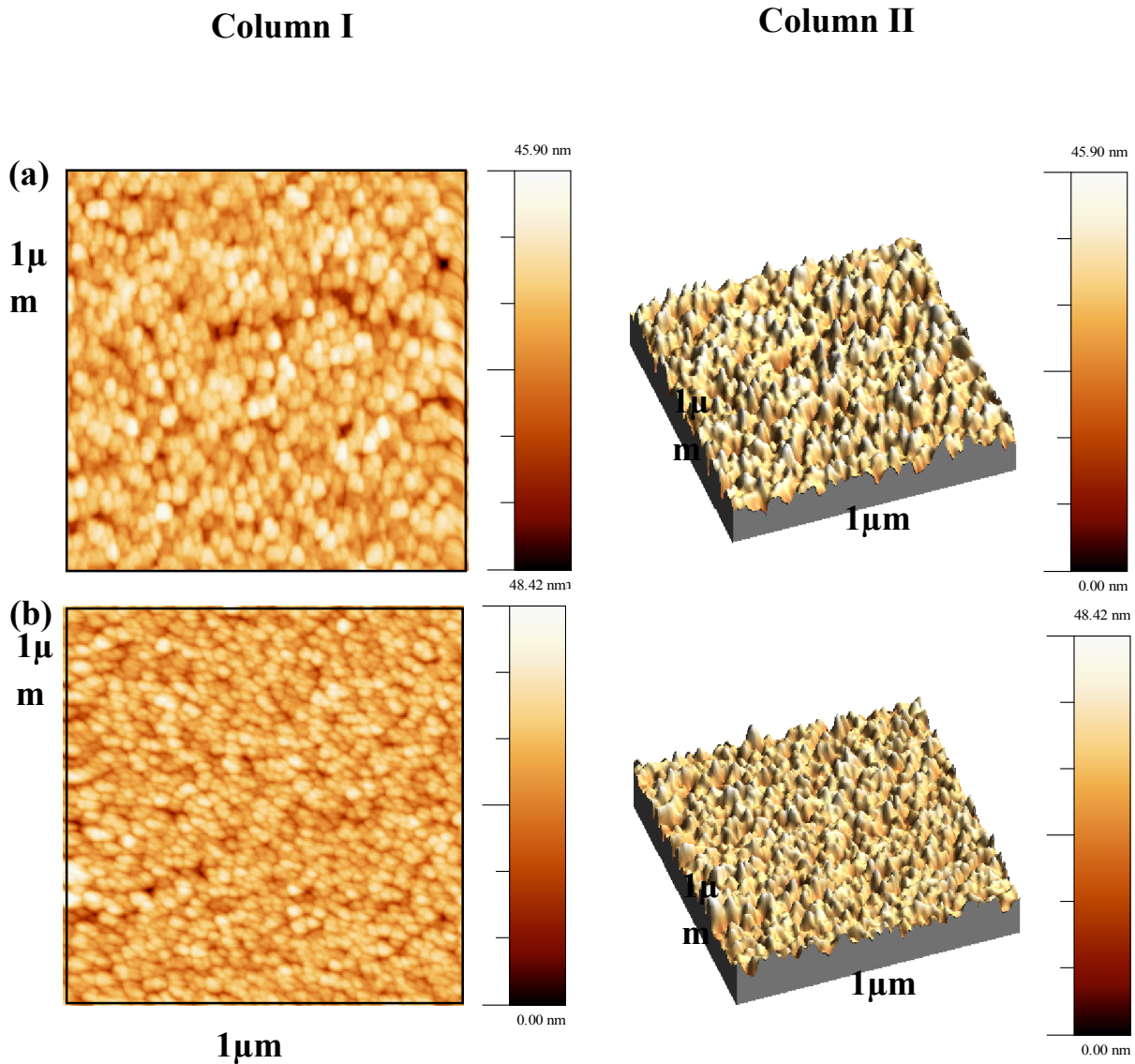


Figure 2. AFM images of manganese nitride thin films. a) monolayer and b) bilayer.

The reason for the smaller grain size of the bilayer structure compared to the other one, is the lack of sufficient opportunity for grain growth in this structure. In fact, because the grain size increases with increasing thickness [21,32], mono-layer structures have a larger grain size than the bilayer structure due to their longer arm length. Average grain size (D_{AFM}), average surface roughness (R_{ave}) and deviation from its mean (Rms) obtained using Nova software, are given in Table (2).

Table 2. Details of experimental results for AISI 304 stainless steel.

	GrainSize (nm)	Average (nm)	Roughness	Rms (nm)	I _{cor} (A/cm ²)	V _{cor} (V(SCE))
AISI 304 SS	-	-		-	12×10 ⁻⁴	-0.62
monolayer	25	15		22	1×10 ⁻⁴	-0.55
bilayer	16	14		16	45×10 ⁻⁶	-0.47

Crystal structure analysis

Figures (3-a) and (3-b) show the X-ray diffraction results of the structures before and after annealing in nitrogen flux, respectively, compared to the XRD spectrum of 304 stainless steel.

As can be seen from the figures, the XRD spectrum of AISI 304 stainless steel has 4 peaks, which are located in $2\theta = 43.7$, $2\theta = 50.7$, $2\theta = 74.8$ and $2\theta = 90.8$, respectively, representing Fe (111) crystal plates γ , Fe (200) $-\gamma$, Fe (220) $-\gamma$ and Fe (311) $-\gamma$.

Figure (3-a) shows in the XRD spectrum of the coated samples, in addition to the peaks related to the substrate, namely the phases, Fe (200) $-\gamma$, Fe (220) $-\gamma$ and Fe (311) $-\gamma$, another peak is located at $2\theta = 43.03$, which represents the phase of Mn (330). (According to the standard card 00-020-0180).

Figure (3-b) shows that the XRD spectrum of the sample coated with mono layer has not changed much due to reheating at nitrogen flux, and only due to grain growth (due to reheating), the Mn (330) peak intensity has increased slightly. But unlike this structure, the bilayer structure has a peak at $2\theta = 40.44$ which indicates the formation of manganese nitride phase and the growth of Mn₄ N (111) crystal plate (according to standard card 00-001-1202).

The reason for the formation of nitride phase for two-layer structures is the small size of the grains, which increases the cross section of the nitrogen gas collision.

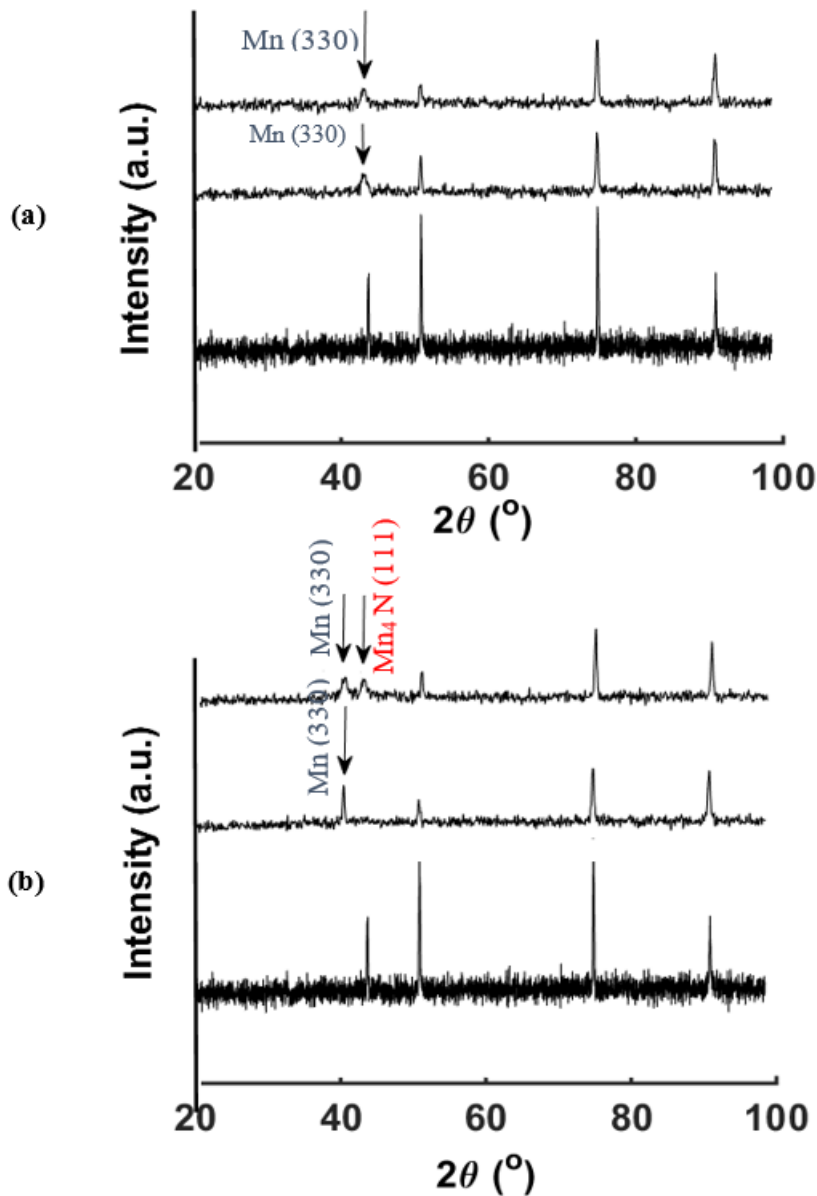


Figure 3. XRD results of manganese thin films a) before and b) after annealing.

Electrochemical analyses

A) Polarization test

Figure (4) shows the polarization curves of steel, monolayer and bilayer structures in 3.5% salt solution. The corrosion current and corrosion potential obtained from these diagrams (using the TOEFL slope) are given in Table 3. The results show that the manganese nitride coating reduces the corrosion current and increases the corrosion potential. It is also clear from the results that the bilayer structure has more corrosion potential and less corrosion current than the other sample. Considering that the corrosion current and corrosion potential control the corrosion rate and corrosion tendency, respectively, so the bilayer coating has a lower corrosion rate and corrosion

tendency than the monolayer thin film (due to the formation of nitride phases). The reason for the higher corrosion resistance, in addition to the formation of the nitride phase is also attributed to the interface effect and the morphology of the bilayer thin film, which is further explained below.

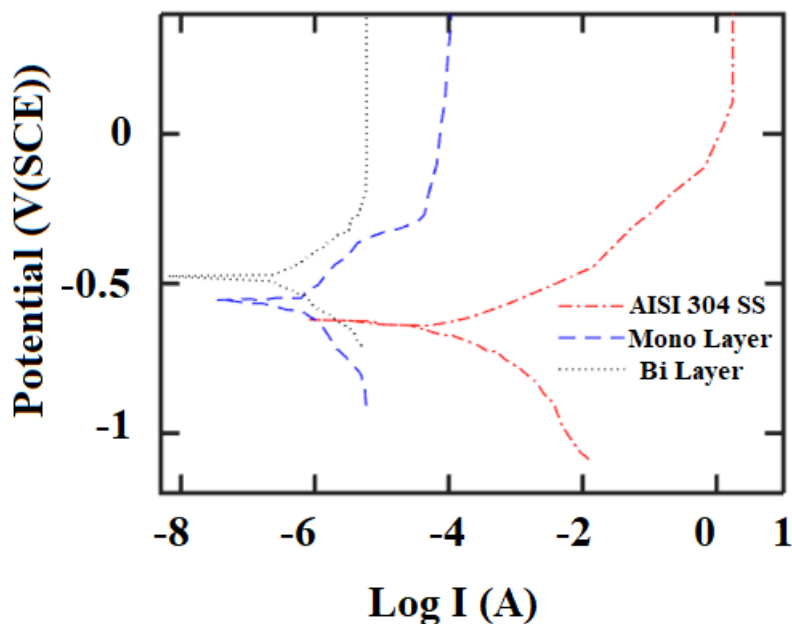


Figure 4. polarization results of samples in the 3.5% NaCl solution.

B) EIS test

Nyquist curves of different uncoated AISI 304 stainless steel, monolayer, and bilayer coatings of manganese nitride on AISI 304 stainless steel is shown in Figure (5). It is clear from the figure that the Nyquist curve of un coated steel has an induction loop that occurs at low frequencies. This inductive behavior indicates the production of corrosion products and the formation of salt on the sample surface through the pitting of aggressive ions on the sample surface [33-37]. Figure 5 shows that the monolayer manganese nitride thin film, although inductive behavior, increases the corrosion resistance. It is also clear from the results that by changing a 110 nm thin layer into two 55 nm layers, this inductive behavior disappears, and corrosion resistance increase. This is due to the presence of nitride phase in this structure. To better investigate the EIS results and the reason for the increase in corrosion resistance by converting the 110 nm monolayer into two 55 nm coatings, the equivalent circuit of these structures was obtained and analyzed.

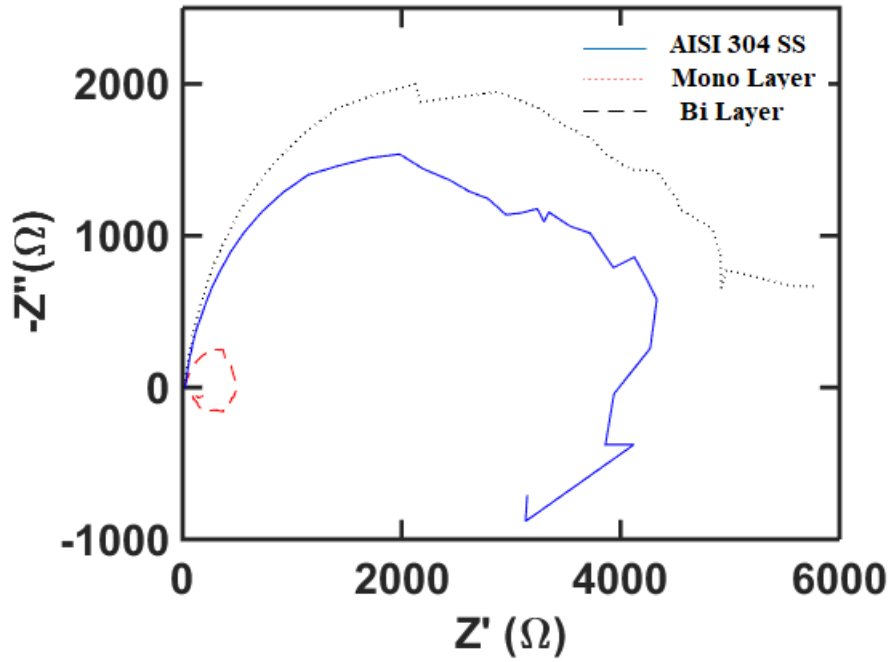


Figure 5. EIS results of samples in the 3.5% NaCl solution.

Figure (6-a) to (6-c) show the equivalent circuit that can be attributed to the sample without any coating, the sample with mono layer coating and the sample with two layers coating respectively. In these circuits, R_s is the resistance of the solution, L is the coefficient related to the inductance behavior, C_{cot} is the capacitance related to the coating, and is seen in incomplete coatings where the solution penetrates the coating. C_{dl} is the dual layer capacitance formed at the metal-coating interface and is given by the following equation [38].

$$C = \varepsilon \frac{A}{d} (5)$$

Where d is the thickness of the coating, A is the area exposed to the solution and k is the dielectric constant of the coating. R_1 is the resistance of the double layer capacitance, R_2 is the resistance of the coating capacitance and R_3 is the resistance of the inductor. Capacitors are not considered ideal due to the surface roughness of them. The parameters α_1 and α_2 indicate how far they are from the ideal capacitor, respectively. Corrosion resistance for different circuits is obtained from the difference between infinite frequency impedance and zero frequency impedance.

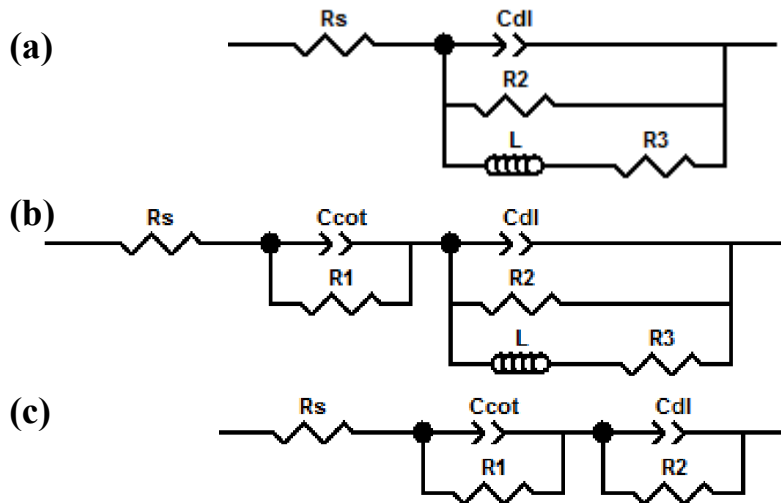


Figure 6. equivalent circuit of a) AISI 304SS, b) monolayer and c) bilayer thin films.

The bod and phase diagrams obtained from experiments and simulations are shown in Figure 7. These figures show the best fit between the experimental and simulation results. Table 4 shows the equivalent circuit quantities obtained using simulations with Zviwe software. The data show that bilayer structure has smaller capacitance relative to monolayer coating. This is due to the small grains of the monolayer thin film in comparison with bi layer structure. Because Ccot is capacitance of a large number of parallel capacitors. The number of these capacitors increases as the grain size decreases. On the other words, the total capacity decreases with grain boundaries increasing. It is also clear from the results that this structure has high electrical resistance compared to the monolayer structure due to better nitride phase formation. Better formation of nitride phase, also eliminates inductance behavior of thin film. So, for bi layer structure Loss of inductive behavior, increase in electrical resistance and decrease in capacitance increase corrosion resistance.

SEM Analysis

To investigate the surface of the samples after corrosion, SEM images of monolayer structure and bilayer structure were studied after polarization test. These images are shown in Figure 7. Comparison of Figure 7(a) with Figure 7(b), which shows the SEM images of monolayer structure and bilayer structure, respectively, shows that the surface of single-layer structure has more degradation than the bilayer structure. So, the bilayer structure of manganese nitride is suitable coating for corrosion protection.

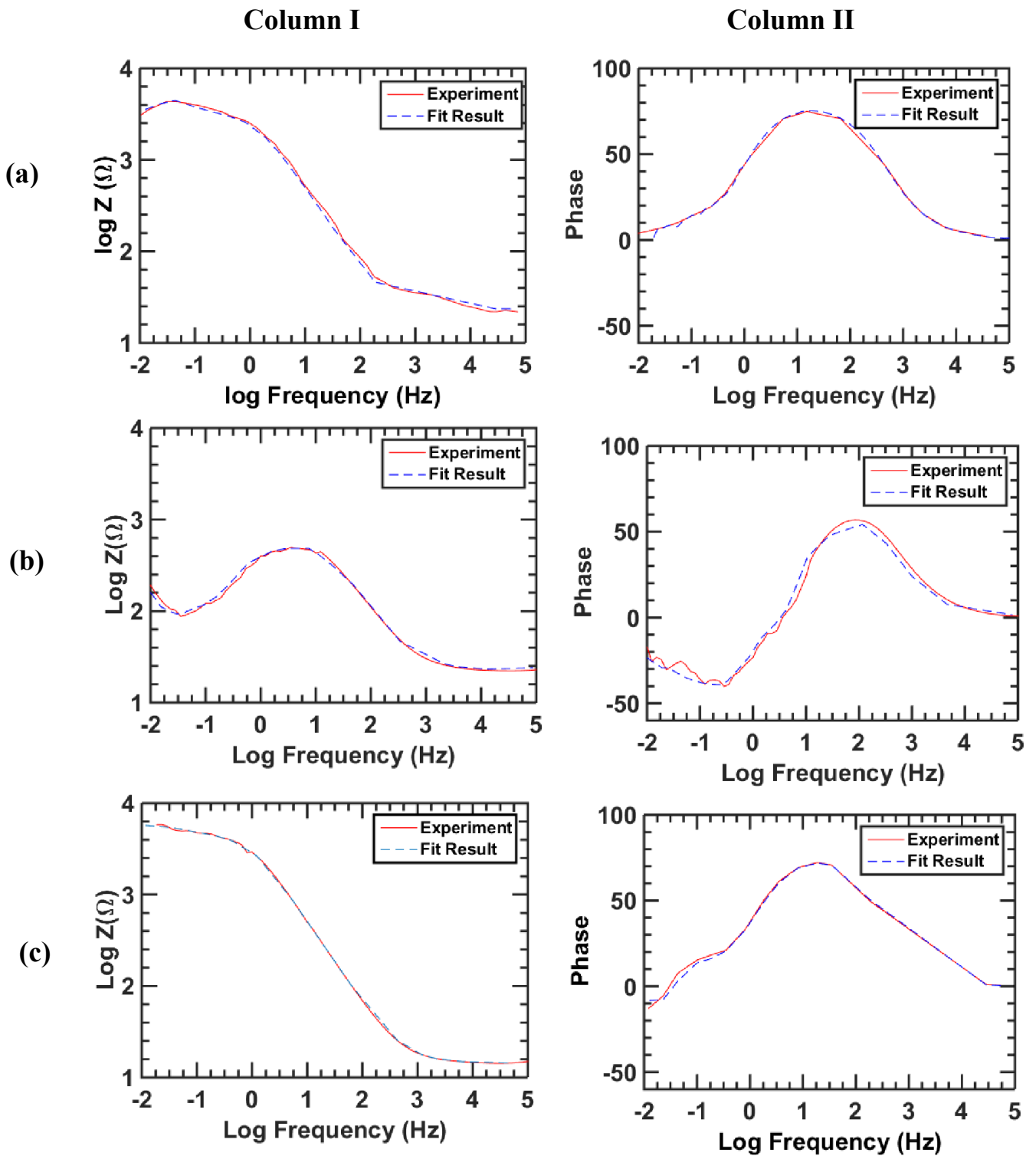


Figure 7. bod (column I) and phase (column II) diagrams of a) AISI 304SS, b) monolayer and c) bilayer thin films.

Table 3.Equivalent circuit quantities.

	steel	monolayer	bilayer
R_s (Ω)	25.7	26.58	27.33
R_1 (Ω)	-	221	352
R_2 (Ω)	98	156	1237
R_3 (Ω)	1387	2534	6021
$C_{co}(F)$	-	16×10^{-5}	2×10^{-5}
$C_{dl}(F)$	37×10^{-4}	21×10^{-4}	15×10^{-4}
α_1	-	0.74	0.8
α_2	.77	0.70	0.84
L	20112	30426	-

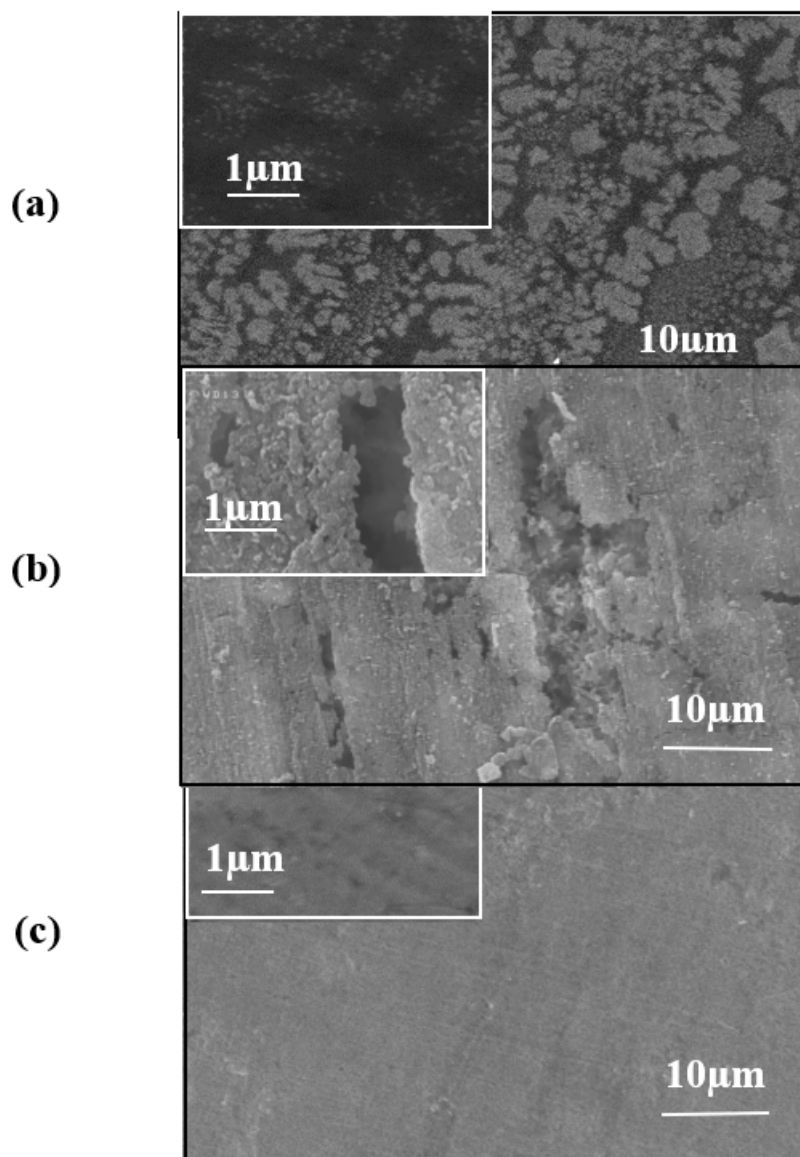


Figure 8. SEM images of a) AISI 304SS, b) monolayer and c) bilayer thin films after corrosion tests.

Conclusion

In order to investigate the effect of geometry and morphology of thin films on corrosion protection of metals, monolayer and bilayer structure of manganese nitride, on AISI stainless steel were coated and their corrosion resistance was studied in 3.5% salt solution. The results showed that the bilayer structure has smaller grains and nitride phase formation occurs better in it. It is observed that induction behavior is not observed for these structures. Also, this structure has a high electrical resistance compared to the monolayer structure, which is due to better nitride phase formation for this structure. In the study of electrical impedance, it was found that bilayer structure has a small capacitance due to the small grain size of the structure. Therefore, due to its high electrical impedance, the bi-layer structure has better corrosion resistance than the mono-layer structure and is suitable coating for corrosion protection.

Acknowledgment

We would like to thank the university of Tehran and university of Mohaghegh Ardabili for their support.

References

- [1] S. E. Ziemniak, M. Hanson, *Corros. Sci.*, 44, 2209 (2002).
- [2] H. Zhang, Y. L. Zhao, Z. D. Jiang, *Mater. Lett.*, 59, 3370 (2005).
- [3] D. H. Mesa, A. Toro, A. Sinatora, A. P. Tschiptschin, *Wear.*, 255, 139 (2003).
- [4] J. D. Crossen, J. M. Sykes, G. A. D. Briggs, J. P. Lomas, *Organic Coatings for Corrosion Control*, 98, 106 (1998).
- [5] H. Savaloni, M. Habibi, *Applied Surface Science.*, 258, 103 (2011).
- [6] C. Liu, G. Lin, D. Yang, M. Qi, *Surf. Coat. Technol.*, 200, 4011 (2006).
- [7] V. H. V. Sarmiento, M. G. Schiavetto, P. Hammer, A. V. Benedetti, C. S. Fugivara, P. H. Suegama, S. H. Pulcinelli, C. V. Santilli, *Surf. Coat. Technol.*, 204, 2689 (2010).
- [8] M. Aparicio, A. Jitianu, G. Rodriguez, A. Degnah, K. Al-Marzoki, J. Mosa, L. C. Klein, *Electrochimica Acta*, 202, 332, (2016).
- [9] D. Pech, P. Steyer, J. P. Millet, *Corros., Sci.*, 50, 1492 (2008).
- [10] A. R. Grayeli, H. Savaloni, *Applied Surface Science.*, 258, 9982 (2012).
- [11] H. Hoche, J. Schmidt, S. Grob, T. T. robmann, C. Berger, *Surf. Coat. Technol.*, 205, 145 (2011).
- [12] A. Dehghanhadikolaei, N. Namdari, B. Mohammadian, B. Fotovvati, E. Research, E. Additive, *J. Sci. Eng. Res.*, 5, 123 (2018).

- [13] P. J. Kelly and R. D. Arnell, *Vacuum*, 56 , 159 (2000).
- [14] K. Baba, R. Hatada, R. Emmerich, B. Enders and G. K. Wolf, *Instrum. Method. B*, 106 , 109 (1995).
- [15] G. F. Huang, L. P. Zhou, W. Q. Huang, L. H. Zhao, S. L. Li and D. Y. Li, *Diam. Relat. Mater.*, 12, 1406 (2003).
- [16]. H. P. Feng, C. H. Hsu, J. K. Lu and Y. H. Shy, *Mater. Sci. Eng. A*, 347, 123 (2003).
- [17] D. Damborenea, J. Navas, C. García, J. Arenas, M. Conde, *Surf. Coat. Technol*, 201, 5751 (2007).
- [18] M. Mathew, E. Ariza, L. Rocha, A.C. Fernandes, F. Vaz, *Tribol. Int.* 41 , 603 (2008).
- [19] K. Dahm, P. Dearnley, *Wear*, 259, 933 (2005).
- [20] P.A Dearnley, G. Aldrich-Smith, *Wear* , 256, 491 (2004).
- [21] B. Fotovvati, N. Namdari, A. Dehghanghadikolaei, *Mater. Res. Express* , 6 12002, (2018)
- [22] L. Liu, P. Yang, C. Su, H. Guo, M. An, *Int. J. Electrochem. Sci*, 8, 6077 (2013).
- [23] D. Fang, X. Li, H. Li, Q. Peng, *Int. J. Electrochem. Sci.*, 8, 2551 (2013) .
- [24] Y. Xin, Ch. Liu W. Zhang, J. Jiang, G. Tang, X. Tian, and P. K. Chua, *Journal of The Electrochemical Society*, 155 ,5 (2008).
- [25] C.S. Wu, Z. Zhang, F.H. Cao, L.J. Zhang, J.Q. Zhang, C.N. Cao, *Applied Surface Science*, 253,3893 (2007).
- [26] K.F. Khaled, *Electrochimica, Acta* ,55, 6523, (2010)
- [27] A. R. Grayeli- corpia, H. Savaloni, M. Habibi, *Applied Surface Science*, 276, 269 (2013).
- [28] F. Abdi, *Chinese Physics B*, 30, 38106, (2021)
- [29] F. Modiri, H. Savaloni, *Journal of Theoretical and Applied Physics*, 14, 21 (2020)
- [30] F. Modiri, H. Savaloni, *Journal of Theoretical and Applied Physics*, 14, 223 (2020).
- [31] F. abdi and H. savaloni, *Optics Communications*, 80, 69 (2016)
- [32] F. abdi and H. savaloni, *Applied Surface Science*, 330, 74 (2015).
- [33] Y. Xin, C. Liu, W. Zhang, J. Jiang, G. Tang, X. Tian, P.K. Chu, *Journal of The Electrochemical Society*, 155, 5 (2008).
- [34] C.S. Wu, Z. Zhang, F.H. Cao, L.J. Zhang, J.Q. Zhang, C.N. Cao, *Applied Surface Science*, 253 3893 (2007).
- [35] D. Fang, X. Li, H. Li, Q. Peng, *Int. J. Electrochem. Sci.*, 8, 2551 (2013).
- [36] L. Liu, P. X. Yang, C. N. Su, H. F. Guo, M. Z. An, *Int. J. Electrochem. Sci.*, 8, 6077 (2013).
- [37] R. Solmaz, G. Kardas, M. C. Ulha, B. Yazici, M. Erbil, *Electrochim. Acta*, 53, 5941 (2008).
- [38] F. Abdi, H. Savaloni, *transactions of nano ferrous metals society of china*, 27, 701 (2017)